

Optical and structural properties of Fe₂O₃-ZnO composite thick films obtained by ultrasonic spray pyrolysis

C. Torres Frausto, M. Zapata Torres, E. Monsibais Silva, E. Valaguez Velasquez, N. Cruz Gonzalez, S. Tomas, M. Meléndez-Lira

Fe₂O₃-ZnO composite gained attention due the several applications like that sensors, photocatalysis, reduction of mercury ions. Fe₂O₃-ZnO composite thick films were prepared by Ultrasonic Spray Pyrolysis on a glass substrate, using 0.1 M aqueous solutions of FeCl₃·6H₂O and ZnCl₂ anhydride. To obtain different elemental concentration of Fe and Zn, we varied the volume of each aqueous solution. The XPS analysis shown that it is possible to modulate the concentration of Zn and Fe in the samples. The X-ray diffraction measurements revealed that the films were composed of different phases corresponding with common stable iron oxides (ZnFe₂O₄, Fe₂O₃) and zinc oxide (ZnO). Results from Raman spectroscopy indicate that Fe₂O₃ vibrational modes are accompanied with new modes due to the presence of additional phases ZnO compounds. The band gaps were evaluated with the help of UV-visible transmittance data using the Tauc model, the results shown a modulation of the band gap values (2.2 eV to 3.2 eV). Theoretical transmittance curves were obtained using the effective medium theory, using the Bruggeman model, these curves showed similar behavior that the experimental transmittance curves.

Introduction

Fe₂O₃ is an important member of the ferrite family that exhibits interesting properties such as stable structure and bandgap in the visible region, it has a more negative valence and conduction band edges than ZnO; thus, a type II band-aligned heterojunction is formed, which can enhance light absorption in the visible range up to 600 nm [1]. The ZnO-Fe₂O₃ composite material has aroused much interest, due to its wide variety of applications; among which we can highlight gas sensors [2], reduction of mercury ions [3], lactate sensor [4], solar oxidation of water [5] and photocatalysis [6]. Various methods have been used to obtain ZnO-Fe₂O₃ composite material such as co-precipitation [7], sol gel [3], hydrothermal [8], and spray pyrolysis [9].

One of the most relevant applications of composite materials or mixed thin films is the possibility of band gap modulation. Several investigations have been reported, where it is possible to vary the bad gap of the composite material ZnO-Fe₂O₃. Güller *et al.* synthesized ZnO-Fe₂O₃ nanocomposites by powder metallurgy [1], they found that the optical properties varied according to status of unmilled Fe₂O₃ and milled Fe₂O₃. Lachheb *et al.* obtained ZnO-Fe₂O₃ nanocomposites [2], and pure ZnO and Fe₂O₃ by sol gel route, they found that the interactions between ZnO and Fe₂O₃ induce a shift of the band gap absorption to longer wavelengths. Sursvanshi *et al.* synthesized Fe₂O₃ and stratified Fe₂O₃/ZnO thin films by chemical spray pyrolysis [3], they obtained that the band gap energy were 2.10 eV and 2.62 eV, respectively.





To obtain the optical properties of composite materials, it is necessary to obtain the dependence of optical constants as a function of the composition. The effective medium theories (EMT), is the most common approach to calculate the optical constants of composite materials in terms of optical constants of the mixing materials and their volume fractions [4]. Two of the most used EMT are Maxwell-Garnet and Bruggeman. The Maxwell Garnet theory is valid for dilute concentration of the inclusions; Bruggeman made a significant improvement through an approximation that

treats the two compounds in symmetrical fashion. There are reported in the literature several investigations where authors used EMT to determinate the optical properties of composite materials [5-8].



To the best of our knowledge, the band gap modulation in ZnO-Fe₂O₃ composites has only been reported in a few works; and for limited concentrations of each material; additionally, the variation of the band gap is not explained or modeled. Undoubtedly, a systematic study in which the concentrations of the various materials are varied is of great interest. In this work pure ZnO and Fe₂O₃, as well as 5 ZnO-Fe₂O₃ composite films, were deposited using the ultrasonic spray pyrolysis technique; the concentration of the elements was varied from the variation of the volumes of the precursor solutions. The samples were characterized using X-ray photoelectron spectroscopy (XPS), X-ray diffraction, Raman spectroscopy, and optical transmission. Using the Bruggeman model, the optical transmission spectra for composite materials were modeled.

Experimental details

ZnO-Fe₂O₃ composite thick films were synthesized on

C. Torres Frausto , M. Zapata Torres , E. Monsibais Silva 
N. Cruz Gonzalez 
Instituto Politécnico Nacional, CICATA Unidad Legaria
Miguel Hidalgo, CDMX, 11500 México.

E. Valaguez Velasquez
Instituto Politécnico Nacional, UPIITA
Gustavo A. Madero, CDMX, 07340, México.

S. Tomas , M. Meléndez-Lira 
Centro de Investigación y de Estudios Avanzados, IPN
Gustavo A. Madero, CDMX, 07360, México.

Received: May 8th, 2023

Accepted: November 17th, 2023

Published: November 22nd, 2023

© 2023 by the authors. Creative Commons Attribution
https://doi.org/10.47566/2023_syv36_1-231101

simple slide microscope glass at 450 °C by ultrasonic spray pyrolysis using high purity FeCl₃·6H₂O and ZnCl₂ anhydrous precursor with distilled water as a unique solvent.

The preparation of each solution is done independently when the appropriate amounts of salts are weighted in a precise analytical balance (step 2) to dilute them in a water beaker to obtain a 0.1 M aqueous solution (step 3). Then (step 4) the solution was put in magnetic agitation at room temperature for 15 minutes on a magnetic stirrer. Every 5 minutes during solution stirring the pH was measured and kept around 4-5 value in all the cases.

Finally, the FeCl₃·6H₂O (FeSol) and ZnCl₂ (ZnSol) solutions, were mixed taking different amounts in percent of the volume, in such a way that the precursor content for one type of salt would be decreasing whereas at the same time for the other salt would increase gradually. Then we labeled the samples as: ZO (prepared with 100 % of ZnSol); ZFO19 (prepared with 90 % of ZnSol and 10 % of Fe Sol); ZFO37 (prepared with 70 % of ZnSol and 30 % of FeSol); ZFO55 (prepared with 50 % of ZnSol and 50 % of Fe Sol); ZFO73 (prepared with 30 % of ZnSol and 70 % of FeSol); ZFO91 (prepared with 10 % of ZnSol and 90 % of FeSol) and FO (prepared with 100 % of Fe Sol).

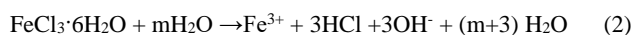
All the Fe-Zn oxide film samples were deposited on microscope glass slide at 450°C, with the ultrasonically (1.73 MHz) vaporized Fe-Zn mixture, using a constant 5 l/min nitrogen flux as carrier gas. The nozzle was set 1 cm above the glass surface which at the same time was supported over a heated stainless-steel plate. The thickness of the samples was measured using a profilometer, the values obtained for each sample were around 1 µm.

The elemental concentration of the samples was obtained by means of X-ray Photoelectron Spectroscopy (XPS) (model K alpha by Thermo Scientific). The general survey was obtained after 30 s of etching with Ar ions. The X ray diffraction (XRD) measurements were carried out using a X ray diffractometer from Brucker with Cu K_α (1.5407 nm) radiation. The samples were scanned in the range 2θ of 15° to 70°. The Raman scattering experiment were carried out at room temperature in a Labram Dilor micro-Raman system, using a 632.8 nm He-Ne laser as excitation source.

The optical transmission of the sample was measured using a Perkin Elmer spectrophotometer model Lambda 40. The transmission spectra of the composite materials were simulated using the Scout software.

Results and discussion

When we mixed the salts with the water, the initial reaction can be described as:



Then we have the cations of Fe and Zn, the behavior of these cations is related to the nature of the molecules species that they form. The simple cation of the element often reacts with the water (hydrolyzes) to form complexes with the hydroxide ion. The complexes are related with the pH of the

solution, and they could be obtained in a Pourbaix diagram. They may be mononuclear or polynuclear, depending on the molar concentration (M); for $M \leq 10^{-3}$ it is expected that the complexes are mononuclear, and for $M > 10^{-3}$ are polynuclear [9]. In our work we used a molar concentration of 0.1 M, then our molecular complexes were polynuclear. For Zn solution, the pH was 4, then if we use the Pourbaix diagram reported by Beverskog *et al.* [10], it is expected that we had Zn²⁺ polynuclear complexes; in the same work they reported that when the Pourbaix diagram is obtained at 300 °C it could be obtained Zn(OH)₂ (aq). For the deposition of the films, the ultrasonic wavelength is applied to Zn solution; then we increased the energy of the system and could be realized some chemical reaction, it is reported that the acoustic cavitation produces intense local heating. On the other hand, Baev *et al.* [11] reported the hydrolysis of iron (III) ions, they reported that for pH bigger than 3 were obtained Fe³⁺ polynuclear hydroxy complexes, for pH between 3 and 3.70 are formed large polynuclear species (containing about 100 iron atoms). Then it is possible that we had polynuclear Zn(OH)₂ (aq) and Fe³⁺ polynuclear species in the droplets of the solutions to be deposited. When the droplets arrive to the heated substrate, we obtained ZnO and Fe₂O₃ grains, and in the interface ZnFe₂O₄.

To obtain an approximate content of each element in the ZnO-Fe₂O₃ composite films, the XPS survey was used in the different samples. The area used for the quantification were the corresponding at the peaks O1s, Fe 2p and Zn 2p. The sensitivity factors for Zn, Fe and O were obtained using a ZnO and Fe₂O₃ standards (from sigma Aldrich, with 99.99 purity); we assume that the common element (Oxygen) for both standards have a sensitivity factor of 1, the sensitivity factors obtained for Zn and Fe were 2.53 and 1.57, respectively. The quantification was done making use of the $C_x = (I_x/S_x)/\Sigma(I_i/S_i)$ formula and the standard areas of the XPS survey spectra. The quantification for all the samples is shown in the Table 1. In the measurements of XPS, the photoelectrons were obtained from the first 10 nm of the material; in our experiments we assumed that the sample is homogeneous in the concentration of the atomic elements in all the thickness.

If it is assumed that the FeSol and ZnSol are immiscible, it is expected that we can obtain a solid solution with the products of the reactions of each solution, Fe₂O₃ and ZnO. The variation of the concentration of the solid solution could

Table 1. Atomic percent concentration in the ZnO-Fe₂O₃ composite films.

Sample	Atomic percent concentration (at%)		
	Fe	Zn	O
ZO	0	50.0±1.0	50.0±1.0
ZOF19	29.0±1.0	14.0±1.0	57.0±1.0
ZOF37	34.0±1.0	12.0±1.0	54.0±1.0
ZOF55	38.0±1.0	4.0±1.0	58.0±1.0
ZOF73	39.0±1.0	2.0±1.0	59.0±1.0
ZOF91	39.0±1.0	1.6±1.0	59.4±1.0
FO	40.0±1.0	0.0	60.0±1.0

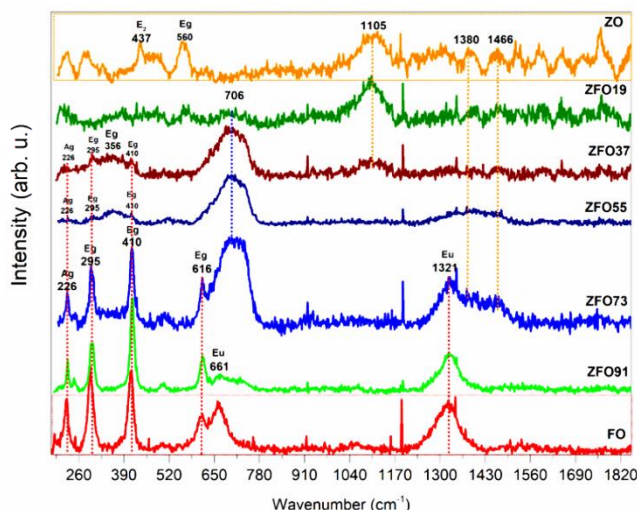


Figure 3. Raman spectra of the different samples.

series of different samples, which the Zn contain is varying in each one of them. It can see at the upper and the bottom in Figure 3 the two Raman spectra corresponding to the pure material of α -Fe₂O₃ and ZnO (labeled as FO and ZO) used as a reference, when the Fe-Zn content changes in them progressively. From the FO spectra the optical normal modes 226, 295, 410, 616, 661, and 1321 cm⁻¹ (A_{1g} + E_g) confirm the existence of the hematite (α -Fe₂O₃) [12]. Bands corresponding with a trigonal D63d space group symmetry. Regarding ZFO91 it is seen the initial grow of a new iron-zinc oxide in 724 cm⁻¹ (ZnFe₂O₄) as this confirm its presence to a very intense peak now at 706 cm⁻¹ as zinc concentration increases (ZFO73, ZFO55 and ZFO37). This iron-zinc oxide, ZnFe₂O₄, belongs to the called spinel (cubic symmetry and space group Fd3m) structure with a general chemical relation AB₂X₄, where A and B are cations and X is the anion.

In Raman spectroscopy only five modes should be observed (A_{1g} + E_g + 3F_{2g}) according with the irreducible representation developing by spinel [13]. However, in our case the only intense peak (706 cm⁻¹) confirm its presence. Coincidentally when the zinc content increases the peaks belonging to hematite (prolonged dotted red line) abates systematically at the same time up to ZFO19 when they disappear completely and only is present the intense peak at 1105 cm⁻¹ together with lowers in 1380 and 1466 cm⁻¹ which are related with the ZO material as the prolonged orange dotted line pointed them. This significant decreasing of peaks and consequently hematite crystalline structure could be due that the ZnO use the hematite structure to build ZnFe₂O₄ so added to this the decreasing in the Fe content promotes that the ZnO cannot find more hematite structure where to accomplish the chemical reaction ZnO + α -Fe₂O₃ → ZnFe₂O₄ that ZnO starts to change its chemical path through CO environment species as indicated by the appearing peak in 1105 cm⁻¹ for ZFO37 and ZFO19. At this point it is evident that peaks 1380 and 1466 cm⁻¹ of the ZnO plus the peak in 1321 cm⁻¹ for hematite are the encounter for the reactive part in the reaction (ZnO + α -Fe₂O₃) while the peak at 706 cm⁻¹ is the result of the product (ZnFe₂O₄) in the

Table 2. Experimental Band Gap for the different samples.

Sample	Experimental Band Gap (eV)
FO	2.31
ZFO91	2.45
ZFO73	2.54
ZFO55	2.57
ZFO37	2.66
ZFO19	3.02
ZO	3.25

same chemical reaction. Overall, the dynamics of the iron-zinc oxide films showed off to principal regions in which when there was enough α -Fe₂O₃-content in the film, the ZnO phase was able to lead the chemical reaction ZnO + Fe₂O₃ → ZnFe₂O₄ that was in good agreement with the XRD results.

The experimental transmittance spectra for the samples are presented curves in Figure 4. It is observed the shift of the absorption edge to shorter wavelengths with respect to an increase of Zn value. Initially for ZFO91, it is observed that its transmittance curve has moved to a shorter wavelength compared with the reference FO composition. This is the same tendency followed for the rest of the iron-zinc concentration as ZFO73, ZFO55, ZFO37 and ZFO19, when their transmittance curves continue going through wavelength shorter for each increment in the zinc-content up to the transmittance corresponding to ZnO. In accord with the XRD and Raman results, it is expected to observe the electronic transitions due to the phases included in the nanocomposite material (ZnO, α -Fe₂O₃ and ZnFe₂O₄). However, the experimental results were not like that, as it can see it again from Figure 4, where the movement of the transmittance curves is accompanied by what it would be apparently one absorption. To have an estimation of the bandgap of the samples, it was considered the model on direct transitions between parabolic bands. The values obtained are presented in Table 2, the results shown that the band gap could be modulated from 2.31 eV to 3.25 eV.

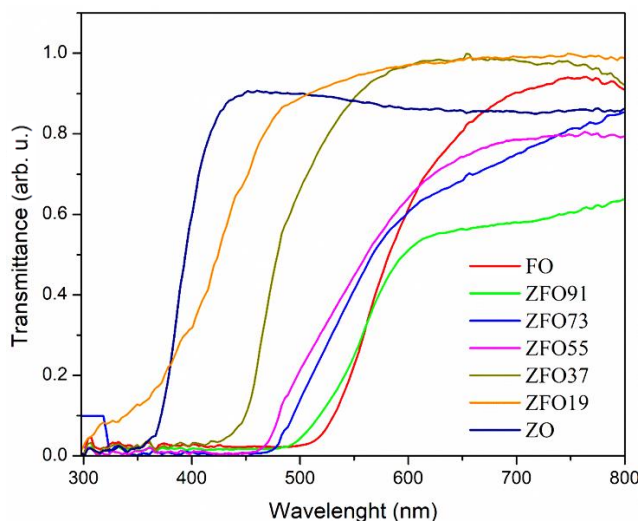


Figure 4. Experimental transmittance spectra of the samples.

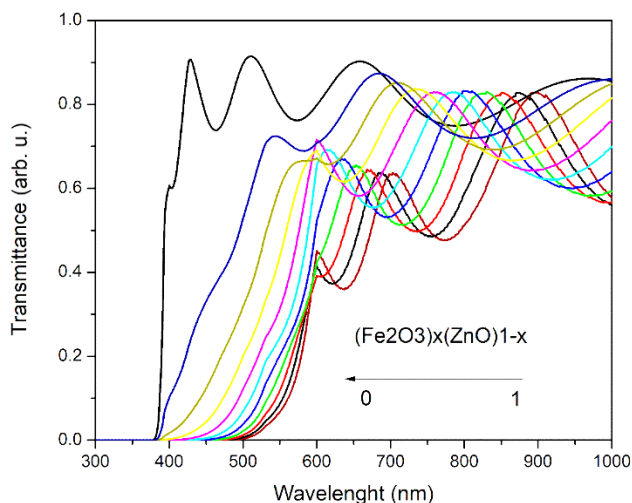


Figure 5. Simulated transmittance spectra of nanocomposite $(\text{Fe}_2\text{O}_3)_x(\text{ZnO})_{1-x}$, for values of x of 0 to 1 in steps of 0.1.

The Scout is a film analysis software that simulate the transmission spectra using the optical constants (refractive index and extinction coefficient) and the thickness. We introduce on the software, the model with the appropriate layer stack; in our simulations were vacuum-composite material-glass-vacuum. If we assume that the grain size is less than the wavelength of the radiation using in the optical transmission experiments. Then we could use the Bruggeman EMT to model the behavior of the transmission measurement of the composite material. We considered the composite material $(\text{ZnO})_{1-x}(\text{Fe}_2\text{O}_3)_x$. The optical constants using were obtained from the Scout database.

In Figure 5 is presented the results of the simulated transmittance curves for different x values, in the range of 0 to 1 in steps of 0.1. It is observed a similar behavior that the experimental transmittance curves for small values of x , but very dissimilar for large x values. It is undoubtedly that more effort is necessary to explain the optical behavior of the composite material, but it is a good rough approximation to modeled using an effective medium theory. It is important to note that the simulated spectra have oscillations due to thickness interference, as it is predicted by the Fresnel equations, these oscillations do not occur in the experimental spectra. This difference is due because in the simulation the software considers that the material is optical flatness; while experimentally the films are rough, so the waves would be dispersed by a rough surface.

To the best of our knowledge, for the first time it is obtained samples of $(\text{ZnO})_{1-x}(\text{Fe}_2\text{O}_3)_x$ for different values of x , with a variation of the absorption edge and tried to give a

qualitative explain to the behavior. On the previous reports [14-17], the authors only obtain the material for a determined relationship between Zn and Fe.

Conclusions

The growth of iron-zinc oxide films in the $\text{ZnO}/\text{ZnFe}_2\text{O}_4/\text{Fe}_2\text{O}_3$ composite structure, by ultrasonic spray at 450°C on simple slide microscope glass, was obtained from a simple aqueous solution with precursors such as $\text{FeCl}_3 \cdot 6\text{H}_2\text{O}$ and ZnCl_2 anhydrous. It was possible to vary the iron-zinc content to obtain a $\text{ZnO}/\text{ZnFe}_2\text{O}_4/\text{Fe}_2\text{O}_3$ composite in form of films with interesting features about the optical respond in the UV-vis electromagnetic region. The results of the simulating transmittance spectra, using the Bruggeman model which gave us a good qualitative behavior with respect the experimental results.

Acknowledgements

This work was supported by SIP-IPN under the project 20231373. The authors thank Marcela Guerrero and Alejandra García for their technical assistance.

References

- [1]. S.H. Güler, Ö. Güler, E. Evin, S. Islak, *Optik* **127**, 3187 (2016).
- [2]. H. Lachheb, F. Ajala, A. Hamrouni, A. Houas, F. Parrino, L. Palmisano, *Catal. Sci. Technol.* **7**, 4041 (2017).
- [3]. R.D. Suryavanshi, K.Y. Rajpure, *J. Photochem. Photobiol. A Chem.* **357**, 72 (2018).
- [4]. J.K. Nayak, P. Roy Chaudhuri, S. Ratha, M.R. Sahoo, *J. Electromagn. Waves Appl.* **37**, 282 (2023).
- [5]. J. Sancho-Parramon, V. Janicki, *J. Phys. D: Appl. Phys.* **41**, 215304 (2008).
- [6]. J.Y. Lu, A. Raza, N.X. Fang, G. Chen, T. Zhang, *J. Appl. Phys.* **120**, 163103 (2016).
- [7]. R.N. Abed, M. Kadhom, D.S. Ahmed, A. Hadawey, E. Yousif, *Trans. Electr. Electron. Mater.* **22**, 317 (2021).
- [8]. A. Heilmann, G. Kampfrath, V. Hopfe, *J. Phys. D: Appl. Phys.* **21**, 986 (1988).
- [9]. C.F. Baes, R.F. Mesmer, *Am. J. Sci.* **281**, 935 (1981).
- [10]. B. Beverskog, I. Puigdomenech, *Corros. Sci.* **39**, 107 (1997).
- [11]. A.K. Baev, E.A. Evsei, *Russ. J. Inorg. Chem.* **55**, 508 (2010).
- [12]. W. Kiefer, *J. Raman Spectrosc.* **38**, 1538 (2007).
- [13]. V. D'Ippolito, G.B. Andreozzi, D. Bersani, P.P. Lottici, *J. Raman Spectrosc.* **46**, 1255 (2015).
- [14]. S. Choudhary, A. Bisht, S. Mohapatra, *Ceram. Int.* **47**, 3833 (2021).
- [15]. X. Li, B. Jin, J. Huang, Q. Zhang, R. Peng, S. Chu, *Solid State Sci.* **80**, 6 (2018).
- [16]. J. Bai, *Mater. Lett.* **63**, 1485 (2009).
- [17]. R.M. Mohamed, A.A. Ismail, *Sep. Purif. Technol.* **266**, 118360 (2021).